DOI 10.35776/MNP.2019.09.02
УДК 628.16:62-278

# The mechanisms of action of inhibitors in the process of calcium carbonate precipitate formation in reverse osmosis apparatus

*Dedicated to the memory of Feliks Nikolaevich Karelin*

**A. G. Pervov[1], A. P. Andrianov[2]**

[1] *Pervov Aleksei, Doctor of Engineering, Professor, Department of Water Supply and Wastewater Disposal, National Research Moscow State University of Civil Engineering 26 Yaroslavskoe Hwy., 129337, Moscow, Russian Federation, tel.: +7 (499) 183-36-29, e-mail: ale-pervov@yandex.ru*
[2] *Andrianov Aleksei, Ph. D. (Engineering), Associate Professor, Department of Water Supply and Wastewater Disposal, National Research Moscow State University of Civil Engineering 26 Yaroslavskoe Hwy., 129337, Moscow, Russian Federation, tel.: +7 (499) 183-36-29, e-mail: AndrianovAP@mgsu.ru*

Knowledge of the mechanism of precipitation of slightly-soluble salts on reverse osmosis membranes is extremely important while choosing measures to prevent it and reduce the flow of concentrate. The conducted studies provided for enunciating a fresh approach to the mechanism of crystalline deposit formation and the role of inhibitors in preventing this process. The development of the experimental technique is based on the idea that the first crystallization phase – crystal nucleation is homogeneous, that is, occurs in dead areas in the concentrate volume at high oversaturation with calcium carbonate. Upon the formation the crystals are removed from the dead areas and settled on the membrane surface like other suspended particles present in the treated water. The results of studying the adsorption of polymer inhibitor molecules on the crystal surface during nucleation and crystalline growth on the membrane are presented. The experimentally obtained dependences of the rate of adsorption of inhibitors on the dose of inhibitors, the rate of formation of calcium carbonate, the rate of nucleation, and on the total surface of the germinal crystals are given. The study of micrographs of crystals showed the dependence of the size and number of crystals on the oversaturation value in the dead area during nucleation as well as on the effectiveness of the inhibitor. A method is presented that allows determining the concentration of dissolved salts in the dead areas of the membrane apparatus and the oversaturation values corresponding to the onset of the crystallization process eliminating the addition and use of various inhibitors.

**Key words:** reverse osmosis, calcium carbonate, mechanism of precipitation on membranes, inhibitor, dead areas, nucleation rate, crystal growth rate, adsorption of inhibitor.

***The authors express gratitude to the Russian Foundation for Basic Research for financial support of the project (RFBR grant No. 19-08-00982 A).***

## INTRODUCTION

The presented article summarizes more than forty years of experience in studying the process of the formation of deposits of slightly soluble salts on reverse osmosis membranes, developing measures to prevent it, and formulating the views on the mechanism of this process. The first domestic experience in the design and practical application of reverse osmosis membrane units for desalination of saline groundwater showed that crystal deposits of slightly soluble salts – calcium sulfate and calcium carbonate – formed rather fast in chambers. This quickly destroyed desalination units due to reduced capacity and selectivity of the membranes. Studies have been conducted to develop measures to prevent scaling. At that time, the main method of combating crystal deposit of calcium carbonate was acidification of the feed water, whereas preventing calcium sulfate deposits was provided by dosing an inhibitor (calcium hexametaphosphate) into the feed water. And if acidification made it possible to solve the problem of the formation of carbonate deposits, then the dosing of inhibitors did not give the expected effect. Moreover, sulfate deposits were formed even in those cases when the concentrate of reverse osmosis plants was not saturated with calcium sulfate, i.e. there was no reason for the formation and growth of crystals.

Studies to elucidate the mechanism of the formation of crystal calcium sulfate deposit in the chambers of reverse osmosis apparatus of the filter-press type were commenced in the 1970s at the Desalination Laboratory of VNII VODGEO under

**Fig. 1. Feliks Nikolaevich Karelin (right) with the employees of the Laboratory for water demineralization and desalination of VNII VODGEO – G. Iu. Assom, A. A. Askerniia, G. A. Zille (1983)**

the supervision of F. N. Karelin (Fig. 1). Studying the surface of membranes removed from the apparatus allowed introducing into the research practice a new concept - dead areas. Due to the uneven flow distribution along the surface of the membranes in the filter-type chamber, areas are formed where the flow rate of water above the membrane is lower than in the main stream. Thus, a concentration polarization layer develops on the surface of the membranes in this area where the concentrations of salt ions can be several times higher than in the main stream above the membrane. The nucleation of crystals occurs precisely in dead areas [1].

F. N. Karelin determined the maximum concentrations of various ions in dead areas. The conditions of mass balance correspond to the state of equilibrium: the amount of salts entering the dead area from the total flow of concentrate equals to the same amount leaving through the membrane. To provide for such an amount of salts passing through the membrane (i.e., the quality of the permeate corresponds to the quality of the feed water) the concentration of salts at the surface of the membrane in the dead area should be equal to:

$$C_з = C_и \cdot 100/R, \qquad (1)$$

where $C_и$ – ion concentration in the feed water, mg/l; $R$ – selectivity of the membrane for these ions, %.

During crystallization of calcium carbonate or calcium sulfate in dead areas the real values of supersaturation achieved in these zones remained unclear. In accordance with the theory of crystallization, the first phase – homogeneous nucleation occurs when supersaturation is achieved. The rate of nucleation (the number of nuclei formed per unit time) depends on the supersaturation [2]. The larger it is, the more nuclei are formed, and the smaller they are. The smaller the size of the crystals in the deposits, the greater the value of supersaturation during their formation should be, whereupon the nuclei start growing. The dependence of the crystal growth rate on the supersaturation value is usually expressed by the formula proposed by Kimura and Okazaki [3], as well as J. Gilron and D. Hasson [4]:

$$dM/dt = (C_р - C_н)^2 K, \qquad (2)$$

where $M$ – specific mass of the deposit per unit of the membrane area; $t$ – time, s; $C_н$ – concentration of the saturated solution, g/cm$^3$; $C_р$ – concentration of the solution close to the membrane, g/cm$^3$; $K$ – constant of the crystal growth rate, cm$^4$/(g·s).

The crystals are washed out from the dead areas deposited on the surface of the membrane and continue to grow receiving calcium from supersaturated solution of the concentrate. Thus, crystal nucleation and crystal growth occur under different conditions.

The mechanism of crystal wash out from the dead area has not been known so far. This is explained in the works of D. Belfort who proposed the theory of "migration" of particles based on the fact that the larger the mass of the particle, the more intense it is entrained by the turbulent flow and washed out from the dead area [5].

Currently, in the world practice of water desalination spiral wound apparatuses with flat membranes are used. The main structural element of the membrane channel in the spiral wound units is a turbulizing mesh forming the channel. As shown by the studies conducted at VNII VODGEO in the 1980s it is the turbulizing mesh that enhances the formation of dead areas and crystal deposits on the membranes. Dead areas appear at the points where the nodes of the turbulizing mesh are pressed against the membrane surface during the apparatus manufacturing (Fig. 2). In dead areas salt concentrations increase 10–20 times compared to the feed water resulting in nucleation. Homogeneous nucleation takes place in the perimembrane layer, whereupon the germinal crystals are washed out from the dead areas and deposited on the membrane surface in the same way as other suspended particles.

Shown in Fig. 2 are microphotographs of the surface of the membrane removed from a spiral wound

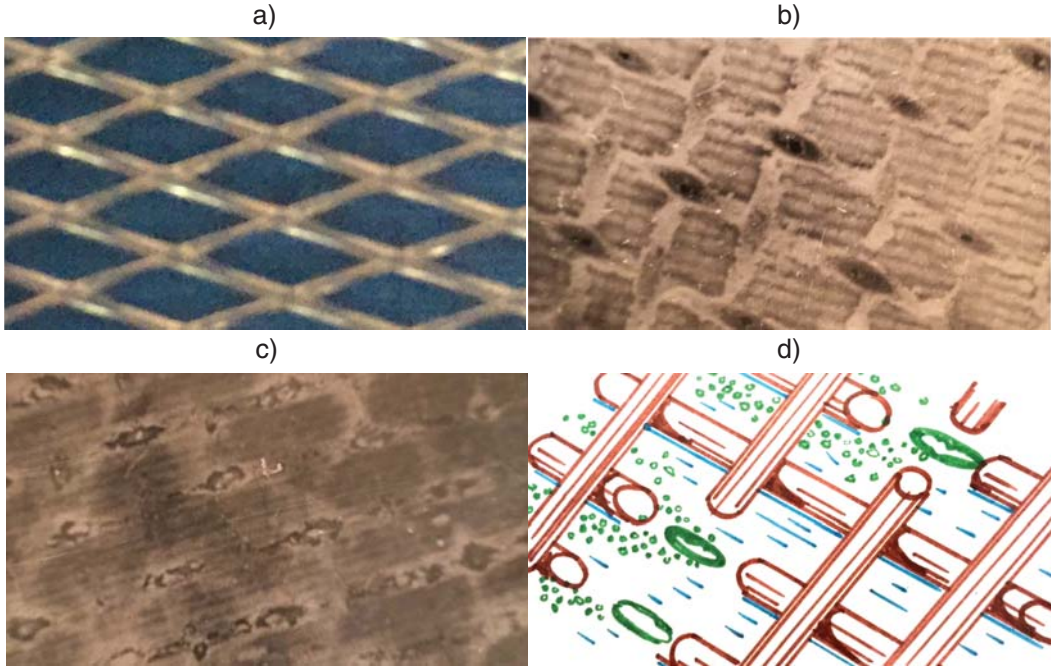


**Fig. 2. Development of dead areas on the membranes in the channels of spiral wound elements**
*a* – turbulizing mesh; *b* – membrane surface at the beginning of scaling; *c* – membrane surface covered with calcium carbonate deposit; *d* – wash out of small crystals from the dead areas and their deposition on the membrane surface

element. Visible are the points of crystal formation and the areas where the suspended small crystals settled. Over time, the entire surface of the membrane becomes coated with a layer of crystals. The crystals in the flow even form buildups around the nodes of the turbulizing mesh (Fig. 2, *c*). The diagram of the formation of germinal crystals in the dead area of the spiral wound element is shown in Fig. 3.

Over the years the rate of sedimentation was studied directly during the operation of industrial apparatuses. The method for determining the rate of scaling was developed on the basis of the mass balance [6]. A comparison of the values provided for determining the effectiveness of measures to prevent scaling, in particular, the effectiveness of various inhibiting agents and to evaluate the effect of their doses on the process of scaling [6].

In modern practice of the preparation of potable and process water from natural underground and surface water sources by reverse osmosis using effective inhibitors is of great importance for the operating costs. As was shown earlier [6], the methods of testing new inhibitors used by various research workers [7–11] do not often provide for the conditions of crystal formation onset. This does not allow the effective use of new inhibitors [12–16]. In some cases, introducing already formed germinal crystals into supersaturated solution with the subsequent determining the crystal growth rate in the presence of various inhibitors is practiced. In other experiments the inhibitor is added to supersaturated solutions; whereupon its effectiveness is determined by the value of supersaturation, at which the onset of nucleation becomes "visible" ("jumps" of calcium or colloidal particles concentrations recorded by the metering instruments). Therefore, it is extremely important to determine the true conditions for the formation of crystals in dead areas.

For research most interesting is determining the degree of supersaturation whereby nucleation begins. In preliminary experiments it was found that the

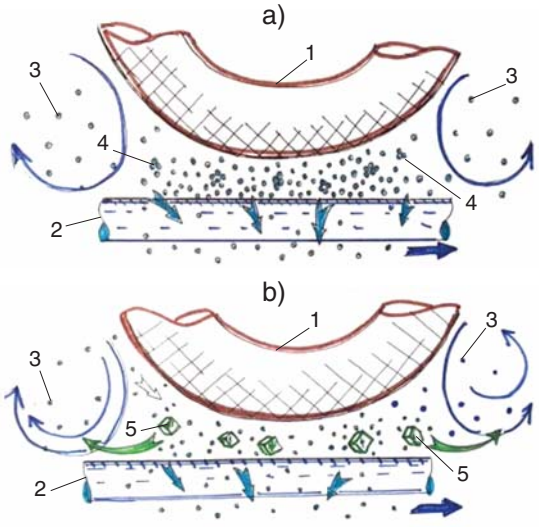


**Fig. 3. Scheme of a nuclei formation process in a dead area**
*a* – feed water concentrating; *b* – formation of crystal nuclei; *1* – turbulizing mesh node; *2* – membrane; *3* – molecules of scaling ions; *4* – nuclei; *5* – crystals

more effective the inhibitor, the smaller the size of the crystals formed [17; 18]. This can be explained not only by the fact that the inhibitor that adsorbs on the surface of the nuclei blocks their further growth. Apparently, the inhibitor delays the progress of the nucleation process itself. Determining the number of crystals formed in the presence of various inhibitors under the same conditions suggested that in the presence of inhibitors the nucleation process ("visible" onset) begins at higher supersaturation values whereby the inhibitor "cannot cope" with blocking the formation of the crystal lattice.

The presented work was aiming at:

determining the composition of water in dead areas and the degree of supersaturation of the solution with calcium carbonate whereby nucleation begins;

experimental determining the dependence of the nucleation rate in a unit volume and crystal growth rate on the level of supersaturation under different conditions (in the presence of different doses of inhibitors);

determining the effect of the composition and doses of inhibitors on the nucleation rate and crystal growth on the membrane surface;

determining the values of the inhibitor adsorption rate during nucleation and crystal growth.

## Experimental methodology

The research program included three series of experiments to determine the dependence of:

the concentration of various ions in permeate and concentrate on the yield of the permeate to simulate the conditions in the dead areas of the membrane apparatus;

the growth rate of the calcium carbonate deposit on the type and dose of inhibitors;

the crystal size on the type and dose of the inhibitor with the purpose of determining the mechanism of its action at the onset of nucleation in the dead area and during crystal growth in the process of deposit accumulation on the membrane.

The experiments were carried out in a laboratory bench; the design is shown in Fig. 4. The bench was operating in a circulation mode with continuous permeate draining. Feed water was supplied to tank *1* with a capacity of 5 l from where water was pumped by pump *2* into the membrane apparatus *3*. Spiral wound elements 1812 with BLN type membranes manufactured by *CSM* (Korea) were used. The membrane area in the element was 0.5 $m^2$. Concentrate from the membrane apparatus was returned to tank *1*, and permeate was transported to a separate tank or discharged into the sewer. The working pressure and concentrate flow rate were controlled using valve *9* mounted on the concentrate line. The operating pressure was 7 ± 0.2 bars. The volume of the recycling concentrate solution was determined by the scale on the tank *1*. Sampling of the recycling solution was made from tank 1, the samples of the permeate from the collection tank *5*. The samples were analyzed for: temperature, conductivity, pH, calcium concentration in water, chloride ions, sulfate ions, total alkalinity.

Conductivity, TDS and temperature were monitored using Cond 730 laboratory conductometer (WNW inoLab), and the pH value was measured with HI 2215 laboratory pH meter (*Hanna Instruments*). Total alkalinity was determined by the titrimetric method according to State Standard 31957-2012;

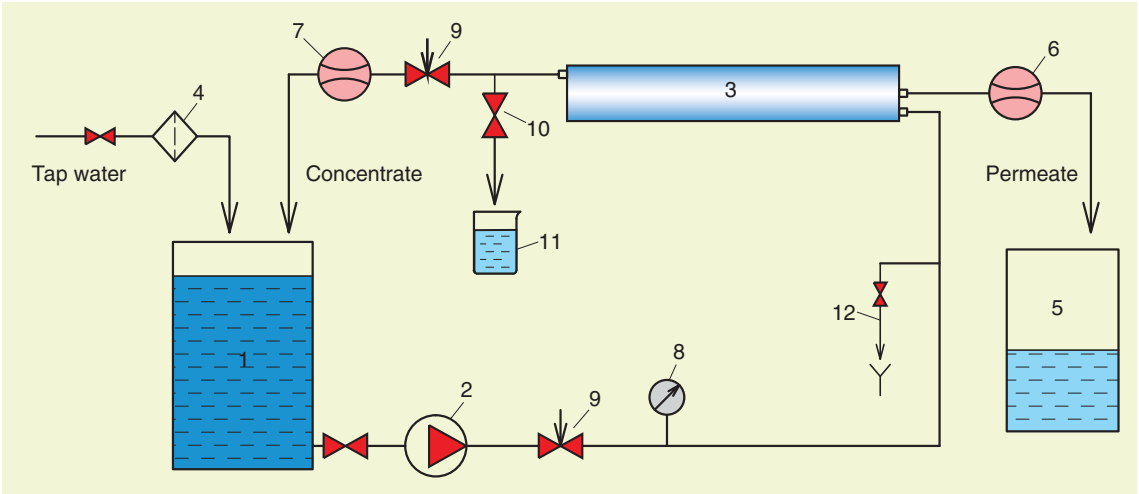


**Fig. 4. Schematic diagram of experimental laboratory unit for water treatment with nanofiltration and reverse osmosis membranes**

*1* – feed water tank; *2* – booster pump; *3* – enclosed spiral wound membrane element; *4* – fine mesh filter; *5* – permeate tank; *6* – permeate flow meter; *7* – concentrate flow meter; *8* – pressure gauges; *9* – adjusting valves; *10* – concentrate drain valve; *11* – wash water collection bucket; *12* – sampler

the concentration of calcium ions was determined by the complexometry according to RD 52.24.403-2007 (Regulatory Guide).

The experiments were conducted on water from the Moscow water supply system. The total dissolved salts (dry residue) was 240–270 mg/l, calcium hardness was 4.5 mg-eq./l, total alkalinity was 100–110 mg/l, the concentration of chloride ions was 25–30 mg/l, and that of sulfate ions – 10–13 mg/ l; pH 7.1.

The concentration factor K is defined as the ratio of the volume in the tank *1* at the initial time to the volume of water at a specific instant of time of the experiment.

Figures 5–7 show the dependences of TDS and concentrations of various ions in the permeate and concentrate of the experimental unit on concentration coefficient K and TDS of the feed water obtained in the first series of experiments. To determine TDS in the dead areas at K value, for example, 1.5, TDS of the concentrate should be determined for the selected value K = 1.5 in the graph of Fig. 6. Given this value, however already as TDS of the permeate, we determine TDS of the concentrate in the graph of Fig. 7. And it will be its value in the dead area. Knowing TDS, pH, and also the concentration of calcium and bicarbonate ions, and using the graphs of Fig. 5–7, it is possible to calculate the supersaturation of the solution with calcium carbonate in the dead areas at the time of the onset of nucleation. The values of supersaturation can determine the rate of nucleation and the role of inhibitors in impeding this process.

In the second series of experiments, the rate of scaling was determined and K values were recorded at which the beginning of scaling was observed in the presence of inhibitors. The amount of calcium carbonate deposit formed on the membranes was determined as the difference between the amount of calcium in tank *1* at the beginning of the experiment and the amount of calcium in the concentrate in tank *1* at a given time [17]. Figure 8 shows the dependences of the amount of calcium carbonate formed versus concentration coefficient K (Fig. 8, *a*) and the duration of the experiment (Fig. 8, *b*). The rate of calcium carbonate formation was determined in accordance with the method developed previously [17] as tangents of the slope to the curve of the dependence of the amount of the deposit formed versus the experiment time. The results are presented in Fig. 8 *c*, in the form of the dependence of the rate of calcium carbonate formation (mg-eq/h) on concentration coefficient K.

In the third series of experiments samples of crystals were prepared and photographed by a scanning electron microscope. A ball valve *10* was installed on the concentrate drain line; with the opened ball

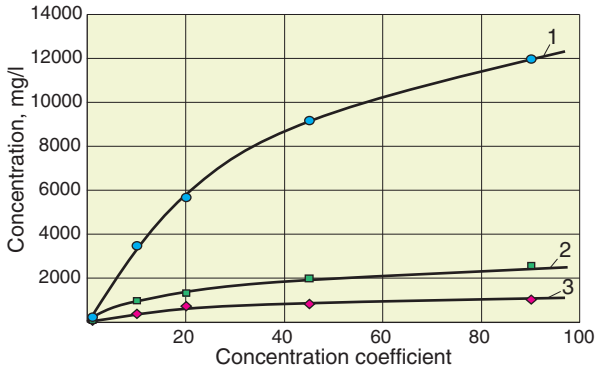


**Fig. 5. Change in TDS (*1*), concentrations of $HCO_3$ (*2*), Ca (*3*) with increasing concentration coefficient**

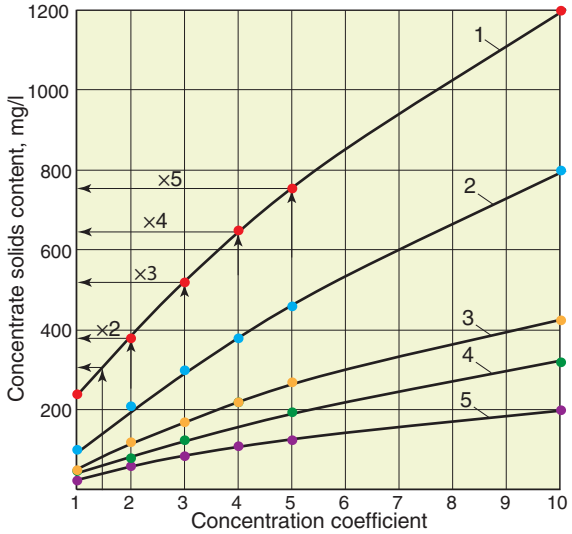


**Fig. 6. Dependence of the concentrate solids content on the concentration coefficient**
*1* – S; *2* – $HCO_3^-$; *3* – $Cl^-$; *4* – $Ca^{2+}$; *5* – $SO_4^{2-}$

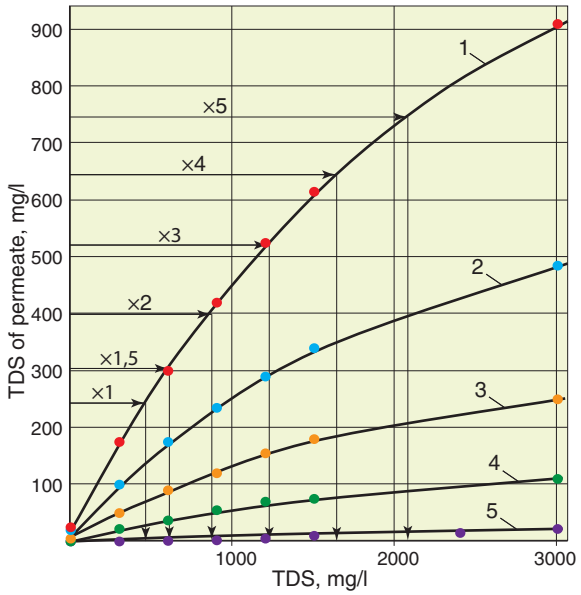


**Fig. 7. Increase in TDS and concentration of different ions in reverse osmosis unit permeate**
*1* – S; *2* – $HCO_3^-$; *3* – $Cl^-$; *4* – $Ca^{2+}$; *5* – $SO_4^{2-}$

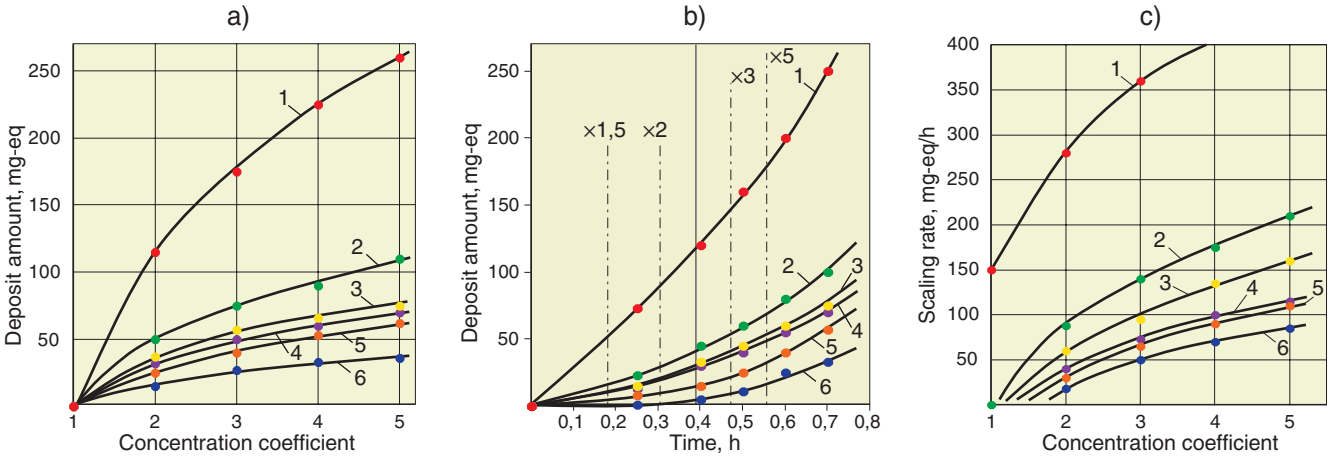


**Fig. 8. Determining scaling rate in the presence of an inhibitor**
*1* – no inhibitor; *2* – PASP-1 at 2 mg/l dose; *3* – PASP-1 5 mg/l; *4* – Aminat-K 5 mg/l; *5* – PASP-1 10 mg/l; *6* – Aminat-K 10 mg/l

valve (with the pump running) the pressure dropped sharply, and the transit flow through the membrane apparatus increased. At the same time the deposit crystals "darted off" from the membrane surface and were washed out by the concentrate stream into the container *11*. The obtained concentrate containing crystals was filtered through MFAS-OS-3 microfilter, the filtration residue was washed with distilled water and dried in the air in an oven at a temperature of 50 °C. Further, the deposit was transferred to carbonic electrically conductive sticky tape and examined by scanning electron microscopy using a microscope with Quanta 250 FEI Company thermal emission cathode and GENESIS APEX 2 EDS energy dispersive X-ray analysis system with APOLLO X SDD EDAX. The observations were carried out at an accelerating potential of 12.5 and 15 kV in the low vacuum mode.

Further analysis of the crystal size and processing of the experimentally obtained data provided for deriving the dependences of the rate of nucleation and crystal growth, and evaluating the effect of inhibitors on this process. In Fig. 9 the pictures of crystals formed from tap water without any inhibitors and in the presence of a PASP-1 antiscalant at doses of 2; 5 and 10 mg/l are presented.

## Discussion of the results

Fig. 8 shows the stages of determining the growth rate of calcium carbonate deposit without an inhibitor and in the presence of PASP-1 and Aminat-K antiscalants. Preliminary studies have shown that Aminat-K is the most effective of the domestic antiscalants [18; 19]. The choice for the new studies of PASP-1 is due to the fact that for today this chemical is the most effective and promising among green phosphorus-free inhibitors [19]. Despite the fact that PASP-1 is inferior in effectiveness to Aminat-K antiscalant [17; 20], its use is justified in projects that do not allow the discharge of nutrients (including phosphorus) present in the membrane unit concentrates that traditionally contain phosphate inhibitors into the surface water bodies [19].

As shown in Fig. 8, the rate of calcium carbonate growth decreases with increasing the antiscalant dose. Fig. 8, *b* shows the time dependences of the

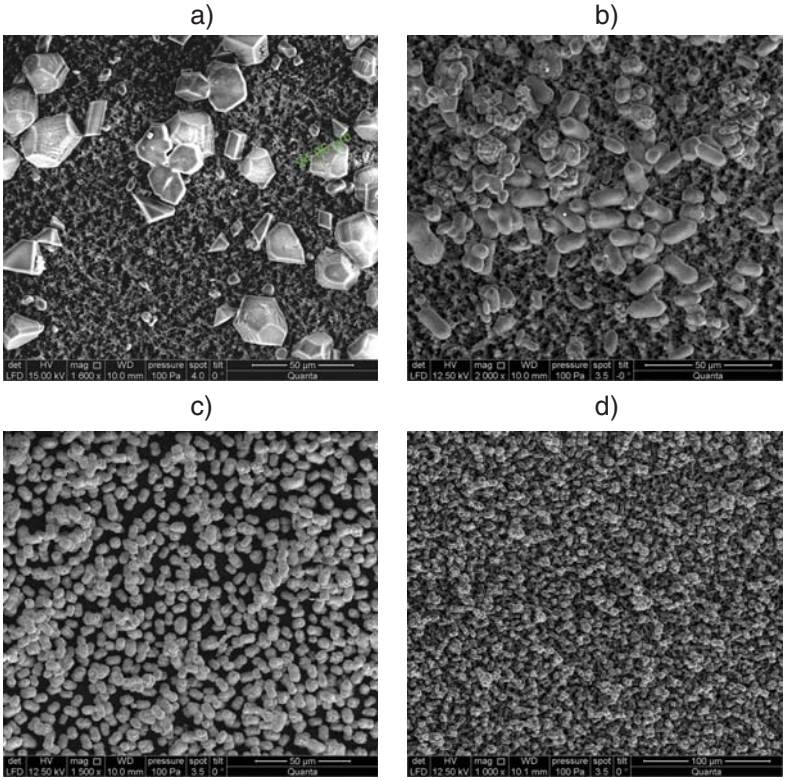


**Fig. 9. Micrographs of calcium carbonate crystals**
*a* – no inhibitor used; in the presence of PASP-1 antiscalant at a dose of: *b* – 2 mg/l; *c* – 5 mg/l; *d* – 10 mg/l

amount of calcium carbonate deposit formed. As can be seen from the figure, at different doses of the inhibitor, the beginning of scaling (K value at which the amount of scale is still zero) corresponds to different K values and, accordingly, different values of solution supersaturation in dead areas. The scaling rate was determined as the tangent of the slope at this point (Fig. 8, *c*). In determining the scaling rate, the authors were guided by the fact that the beginning of crystal yielding corresponds to a point on the abscissa axis (K value) that corresponds to the beginning of scale formation. At this point in Fig. 8, *c*, the rate of onset of crystal yielding was determined. Thus, the obtained values of the scaling rate correspond to the rate of the first phase of crystallization - homogeneous nucleation. Figure 9 shows that the more effective the inhibitor is used and the lower the scaling rate, the smaller the size of the crystals formed.

As shown by the results of previous studies [20], with an increase in the rate of calcium carbonate formation, the rate of adsorption of the inhibitor on the crystal surface increases. Fig. 10 shows the results of measurements of the rate of adsorption of an acrylic fluorescent antiscalant to the surface of crystals [20]. Due to the fact that the measurement of inhibitor concentrations in water is an extremely complicated procedure, and the efficacy of PASP-1 and that of PAA-F1 fluorescent antiscalants are very close, we used the data obtained in [20] to discuss the mechanism of their action in this article. As can be seen from Fig. 10, with an increase in the inhibitor dose, its adsorption rate on the crystal surface also increases. The rate of adsorption of the inhibitor at the initial moment of formation of calcium carbonate deposit corresponds to the rate of its adsorption at the time of initiation of nucleation.

The presented graphs of the dependence of

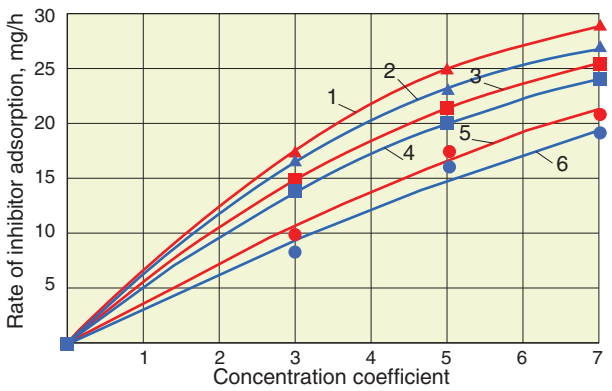


**Fig. 10. Results of determining the adsorption rate of Aminat-K and PAA-F1 antiscalants on crystalline deposit depending on the concentration coefficient**
*1* – Aminat-K at a dose of 7 mg/l; *2* – PAA-F1 7 mg/l; *3* – Aminat-K 5 mg/l; *4* – PAA-F1 mg/l; *5* – Aminat-K 3 mg/l; *6* – PAA-F1 3 mg/l

the scaling rate on the concentration coefficient represent a summarized description of the process of crystalline calcium carbonate accumulation on the membranes. As already shown earlier [1; 6], germinal crystals formed in dead areas, are removed from them and deposited on the surface of the membranes. During the operation of the membrane apparatus, the formation of crystals and their growth on the surface of the membranes occur simultaneously. This significantly complicates the separate description of the nucleation and crystal growth processes, as well as the study of the role of inhibitors in their inhibition.

The results obtained provide for formulating the basic principles of the mechanism of formation of calcium carbonate in the dead areas of membrane apparatus. Homogeneous nucleation occurs in dead areas while a preset level of solution supersaturation with calcium carbonate is reached. Each value of supersaturation corresponds to a certain value of the rate of nucleation – the number of nuclei formed per unit time in a unit volume. It is of interest that this value of the nucleation rate is maintained throughout the experiment for different values of the permeate yield (K value) and for different values of the supersaturation of the feed water. The proof of that is the type of crystals obtained and the uniformity of their sizes.

As can be seen in Fig. 9, the higher the dose of the inhibitor, the finer crystals are formed. Otherwise, at different values of supersaturation in the dead areas of the apparatus, crystals of different sizes would continuously form: the greater the supersaturation at the beginning of nucleation, the smaller crystals in large quantities will form. Moreover, the dependence of the amount of deposit formed on the concentration ratio (Fig. 8, *a*) would appear to be constantly increasing, since with an increase in supersaturation in dead areas, the number of nuclei formed would increase, and with an increase in K, the amount of deposit would grow much faster.

This assumption can be explained as follows: the formation of germinal crystals occurs in dead areas upon reaching a preset level of supersaturation. Hereupon, the nucleation phase begins, the rate of which remains constant during the experiment with various degrees of supersaturation of the feed water. This is explained by the fact that upon reaching a preset level of supersaturation in the dead area, the formation and growth of nuclei begins. With an increase in supersaturation (an increase in the concentration of calcium and carbonate ions), these ions merge into the crystal lattice since the process of crystal formation and growth is already underway. New crystals do not form.

Of interest are the dependences of the growth

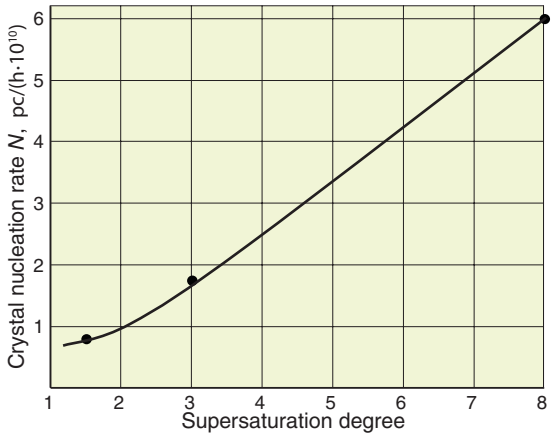


**Fig. 11. Dependence of crystal nucleation rate on the supersaturation degree**

rate of calcium carbonate deposit on K; the growth rate of the deposit on supersaturation with calcium carbonate for different doses of inhibitors; and the rate of homogeneous nucleation on supersaturation. Such dependences make it possible to understand the mechanism of action of inhibitors [20]. To determine the nucleation rate, the pictures of crystals formed from tap water without the use of an inhibitor, as well as at doses of inhibitor 2; 5 and 10 mg / l were used (Fig. 9). Knowing the crystal size, the volume and mass of one crystal were determined, and, knowing the deposit amount, the number of crystals was determined. The rate of small crystal formation depends on the supersaturation in the dead area; whereas its value corresponding to the beginning of crystal formation is determined based on the data in Fig. 6 and 7 and in each case corresponds to the value of K, at which nucleation begins.

Shown in Figure 11 is the dependence of the nucleation rate *N* on the level of supersaturation. The calculation of the supersaturation values carried out in accordance with the method described in [21] is presented in Table 1, the results of determining the parameters of crystals - in Table 2. The degree of supersaturation as the ratio of the product of the concentrations of calcium and carbonate ions to the product of calcium carbonate solubility ($PR_{CaCO_3}$) was determined in accordance with the procedure described in [21]. Concentrations of carbonate ions were calculated from the ratio of the concentration of carbonate ions to bicarbonate ions $S = [CO_3]/[HCO_3]$. The value of *S* was determined from the nomogram from [21]. The calculation results are shown in Fig. 12.

Of interest is the dependence of the inhibitor adsorption rate on the surface area of germinal crystals formed during the nucleation phase at the very beginning of the process. Fig. 13 presents the results of determining the adsorption rate of PASP-1 and Aminat-K antiscalants depending on the crystal surface area corresponding to the previously calculated values of *N*. As can be seen from Fig.13, Aminat-K antiscalant provides for higher adsorption rates than PASP-1 at similar doses. Having plotted the dependence of the adsorption rate (for different K values) on the dose of the inhibitor, it becomes apparent that different inhibitors provide for different adsorption values on different crystal areas. Stronger

*Table 1*

| No. | K | Ca, mg-eq/l | $HCO_3$, mg-eq/l | pH | TDS, mg/l | PR | $[CO_3]/[HCO_3]$ | $CO_3$ | $[Ca][CO_3]/PR$ | K |
|---|---|---|---|---|---|---|---|---|---|---|
| 1 | 1 | 4.5 | 2 | 7.3 | 200 | | 0.01 | 0.02 | 20 | |
| 2 | 2 | 8 | 3.2 | 7.6 | 380 | | 0.015 | 0.04 | 100 | |
| 3 | 3 | 12 | 6 | 7.9 | 520 | $5.22 \cdot 10^{-9}$ | 0.018 | 0.1 | 200 | |
| 4 | 4 | 18 | 7.4 | 8 | | | 0.02 | 0.14 | 540 | |
| 5 | 5 | 20 | 9 | 8.2 | 650 | | 0.03 | | 1000 | |
| | 15 | 40 | 40 | 9 | 4600 | | 0.3 | 12 | 1.2·105 | 1 |
| | 20 | 70 | 60 | 9.2 | 5700 | | 0.4 | 24 | 3.3·105 | 1.5 |
| | 30 | 100 | 80 | 9.3 | 7300 | | 0.5 | 40 | 7.8·105 | 2 |

*Table 2*

| Inhibitor dose, mg/l | Average size, μm | Volume of crystals, $m^3$ | Crystal mass, kg | Number of crystals, pc. | Mass of crystals, mg-eq | Surface area of crystals, $m^2$ | Total surface area of crystals, $m^2$ | Crystal growth rate, pc/h |
|---|---|---|---|---|---|---|---|---|
| 2 | 7 | $35 \cdot 10^{-17}$ | $35 \cdot 10^{-14}$ | $1.6 \cdot 10^{10}$ | | $30 \cdot 10^{-11}$ | 4.8 | $0.8 \cdot 10^{10}$ |
| 5 | 5 | $12.5 \cdot 10^{-17}$ | $12.5 \cdot 10^{-14}$ | $3.2 \cdot 10^{10}$ | $5.6 \cdot 10^{-3}$ | $15 \cdot 10^{-11}$ | 5.8 | $1.6 \cdot 10^{10}$ |
| 10 | 3 | $2.7 \cdot 10^{-17}$ | $2.7 \cdot 10^{-14}$ | $12 \cdot 10^{10}$ | | $5.4 \cdot 10^{-11}$ | 6.5 | $6 \cdot 10^{10}$ |

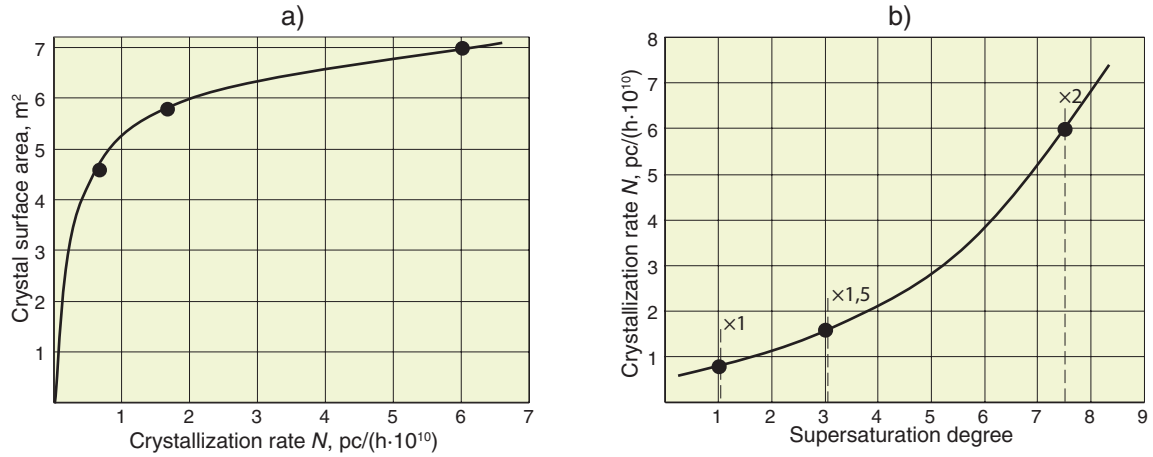


**Fig. 12. Dependences of the crystal surface area on *N* (*a*) and *N* on the supersaturation degree (*b*)**

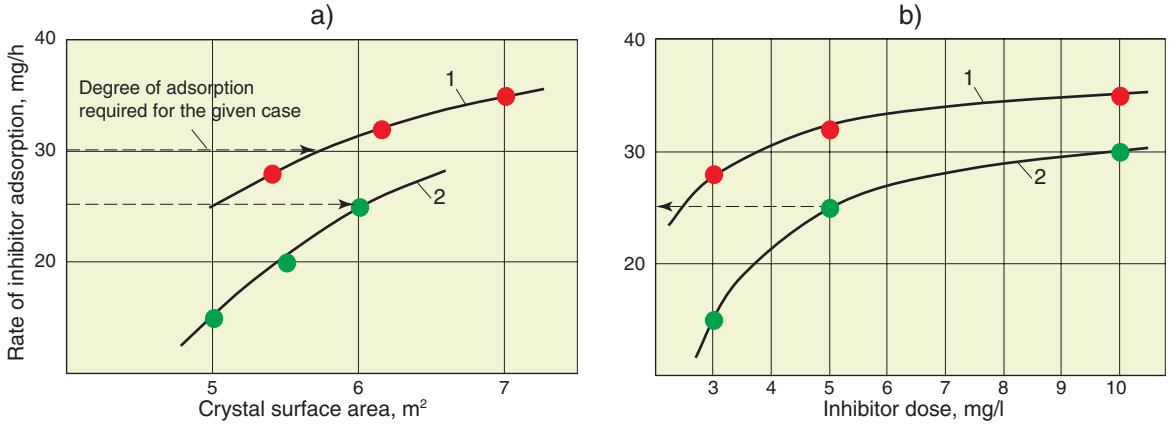


**Fig. 13. Dependence of the rate of inhibitor adsorption on the crystal surface area (*a*) and inhibitor dose (*b*)**
*1* – Aminat-K; *2* – PASP-1

Aminat-K antiscalant at a dose of 10 mg/l ensures the adsorption of the inhibitor on the crystal surface corresponding to the onset of crystallization at K = 1.5; whereas PASP-1 inhibitor at a dose of 10 mg/l cannot provide for such a value.

Thus, using the data in Fig. 13 one can check the effectiveness of the inhibitor: determine the supersaturation and *N* values that correspond to the onset of crystallization at a preset value of K, the required rate of adsorption of the inhibitor, and also check the inhibitor dose that can provide for this rate. Fig.13 also explains why Aminat-K antiscalant ensures the same scaling rate at doses of 2–7 mg/l [20], and PASP-1 antiscalant provides for various scaling rates. Strong Aminat-K antiscalant at all doses, even at a small one of 2 mg/l provides for a higher adsorption rate than PASP-1 and sufficient to block nucleation.

As it turned out, during the operation of the reverse osmosis apparatus two processes occur simultaneously in the membrane channel: the formation of crystal nuclei in the dead areas and then crystal wash out from the dead areas, their deposition on the membrane surface and further growth in the supersaturated solution. The main goal set by the authors of the article was developing a description of each process. For this, a quantitative description of nucleation should be "separated" from the growth of already formed crystals that are described by completely different dependencies. Thus, it is necessary to obtain quantitative dependences of the mass of formed calcium carbonate on time during nucleation and crystal growth.

Nucleation begins in dead areas when a specified level of supersaturation is reached. Therefore, the obtained values of the scaling rate (Fig. 8, *в*) at K values corresponding to the onset of scaling conform to the nucleation rate. Thus, the main "driving force" of the process of deposit accumulation is the continuous "generation" of crystals in dead areas. To imagine how nuclei grow during the experiment we take only the number (mass) of nuclei formed at the beginning of the experiment while the value of K changed from 1 to 2. Next we calculate the number of nuclei that formed when K changed from 2 to 3, from 3 to 4, from 4 to 5. This amount was determined based on the nucleation rate multiplied by the time of K changing from 2 to 3 and so on.

Figure 14, *a* represents the dependences of the

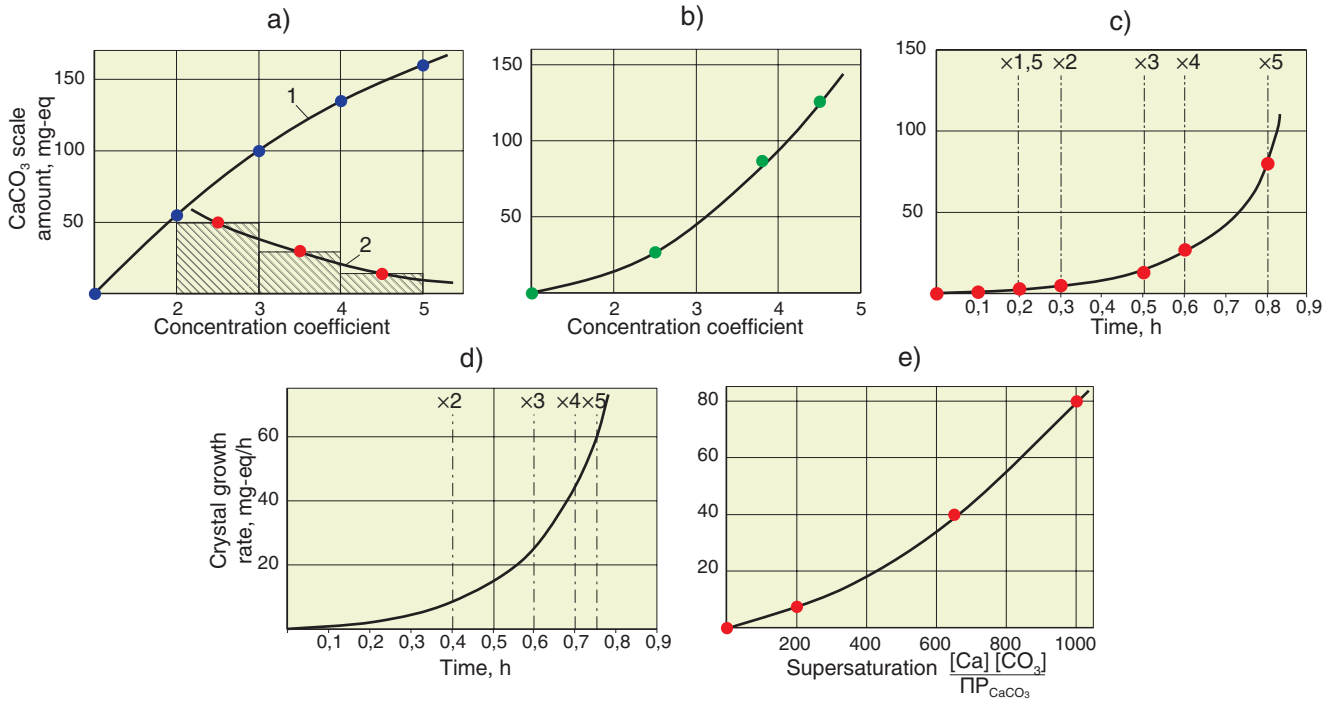


**Fig. 14. Dependences of $CaCO_3$ scale amount on the concentration coefficient (*a*, *b*) and time (*c*); growth rate of the crystals deposited on the membrane surface on time (*d*) and supersaturation (*e*)**
*1* – total deposit mass; *2* – nuclei mass

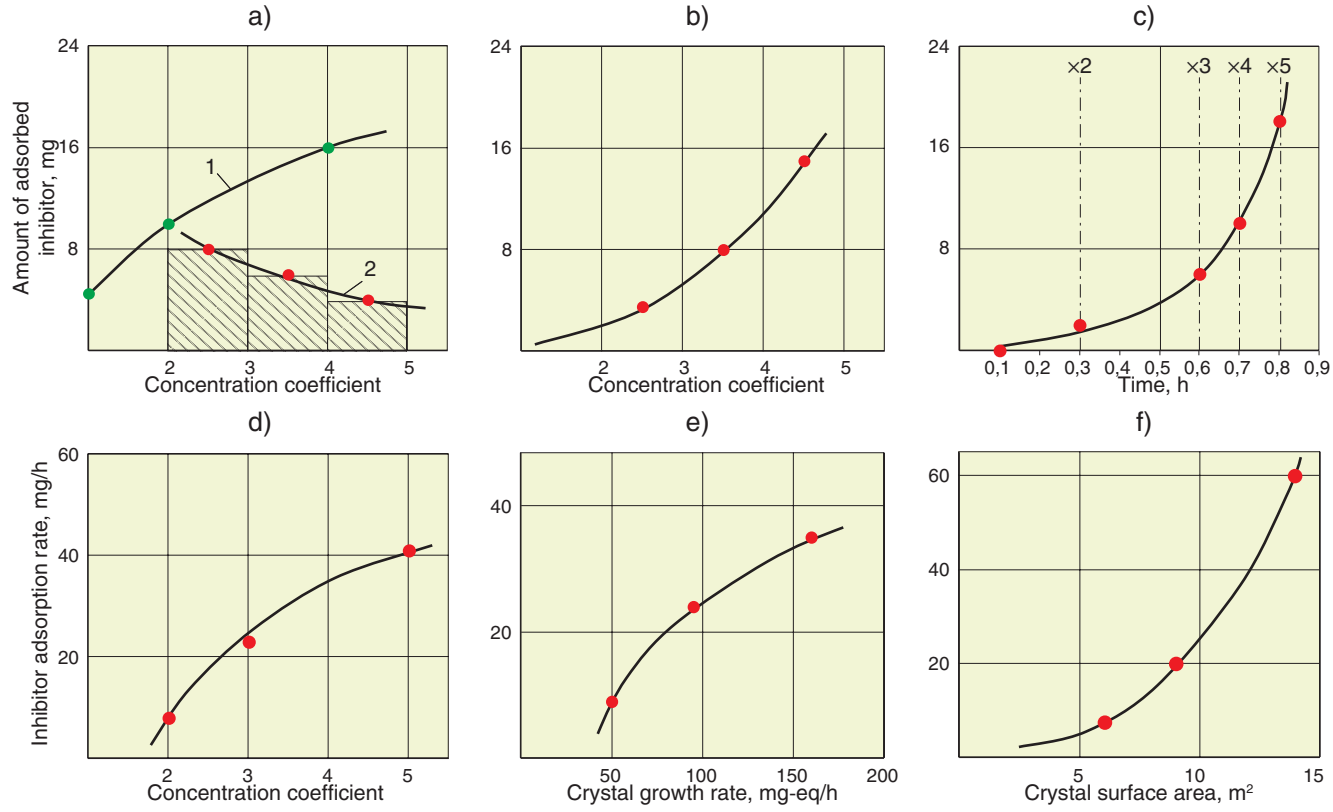


**Fig. 15. Dependencies of the amount of adsorbed inhibitor on the concentration coefficient (*a*, *b*) and time (*c*); the rate of inhibitor adsorption on calcium carbonate crystals on the concentration coefficient (*d*), crystal growth rate (*e*) and crystal surface area (*f*)**
*1* – total mass of adsorbed inhibitor; *2* – mass of inhibitor adsorbed on crystal nuclei

amount of calcium carbonate deposit (Fig. 8, *a*) and the number of germinal crystals formed during the experiment on K. To obtain the dependence of the mass of calcium carbonate formed on germinal crystals on the membrane surface during the experiment (Fig. 14, *a*), it is necessary to subtract the value of the deposit mass of the lower curve from the deposit mass of the upper curve. In Fig. 14, *b* the obtained dependence of the mass of calcium carbonate formed during the experiment on germinal crystals deposited on the membrane during the period of K changing from 1 to 2 is shown. Further, knowing the amount of calcium carbonate formed, we can determine its dependence on the time of the experiment, as shown in Fig.14, *c*, as well as the growth rate of these crystals versus time (Fig. 14, *d*). And, finally, it is possible to plot the main dependence of the crystal growth rate against the level of solution supersaturation with calcium carbonate (Fig. 14, *e*).

To identify the mechanism of action of inhibitors during crystal growth obtaining the values of their adsorption rate depending on the level of supersaturation and the crystal growth rate is needed. Similarly, with the description of the crystal growth rate on the membrane (Fig. 14) the dependence describes the rate of inhibitor adsorption on the crystal surface on the rate of calcium carbonate formation (Fig. 15) and on the degree of supersaturation. Processing the dependencies shown in Figs. 10 and 13, allows showing the dependence of the adsorption rate of the inhibitor during crystal growth and on the values of K, supersaturation, dose of the inhibitor and the surface of the growing crystals.

Figure 15 shows the stages of plotting the dependences: the amount of the adsorbed inhibitor on the crystals formed at the beginning of the experiment on K (*a*, *b*) and on the duration of the experiment (*c*); adsorption rates on K (*d*), on the crystal growth rate (*e*), and on the surface area of the crystals (*f*). Dependencies were constructed for the case of using Aminat-K antiscalant at a dose of 5 mg/l [20].

Based on the work done the mechanism of action of inhibitors in dead areas can be explained. The more effective the inhibitor is used, the higher K concentration coefficient is at which scaling begins: that is, at a higher concentration in dead areas and at a higher degree of supersaturation. At a higher degree of supersaturation the nucleation rate (the number of germinal crystals per unit time) is higher. The presence of inhibitor in the feed water "impedes" the nucleation process – the formation of a "noticeable" amount of germinal crystals. The amount of the inhibitor present in water plays an important role here: with a small degree of supersaturation and a small amount of generating nuclei, their growth is completely blocked by the inhibitor. At a high degree of supersaturation and the formation of a large number of nuclei, the dose of the inhibitor may be "not enough" to block their growth, therefore, the process of nucleation begins.

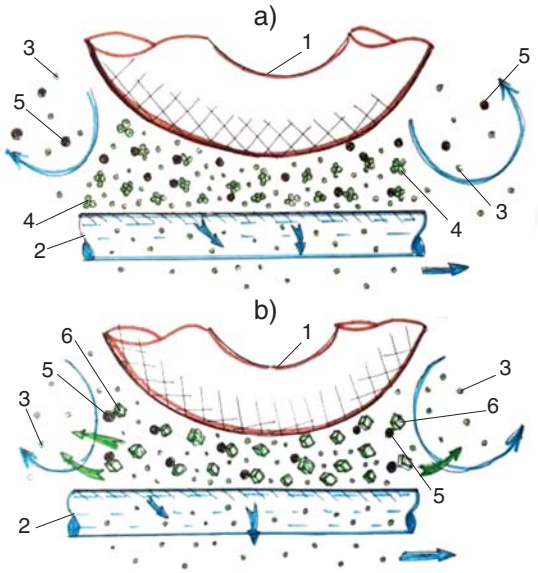


**Fig. 16. Scheme of nucleation process in a dead area in the presence of inhibitor**

*a* – concentration of feed water; *b* – nucleation; *1* – turbulizing mesh node; *2* – membrane; *3* – molecules of scaling ions; *4* – nuclei; *5* – inhibitor molecules; *6* – crystals

The process scheme of crystal formation in dead areas in the presence of an inhibitor is presented in Fig.16.

## CONCLUSIONS

Crystal formation starts in dead areas at the same supersaturation level notwithstanding the concentration of hardness salts in the concentrate of a reverse osmosis unit.

The presence of the inhibitor increases the degree of supersaturation where nucleation begins. Therein the number and dimensions of germinal crystals depend on the degree of supersaturation: the higher supersaturation, the smaller crystals are formed in vast numbers.

Different inhibitors provide for different adsorption rates on the same area of the formed crystals at the same supersaturation values. Therefore, more "strong" inhibitors provide for a greater amount of adsorbed material on the area of the formed crystals blocking their growth. And in case of using "weak" inhibitors their adsorption capacity is not enough to block the crystals formed.

The presence of an inhibitor impedes the nucleation process in the dead area. At a low degree of supersaturation and a small amount of generating nuclei their growth is completely blocked by the inhibitor. At a high degree of supersaturation and

formation of a large number of nuclei the dose of the inhibitor may not be sufficient for adsorption on a large area of the crystal surface and blocking the growth of crystals; therefore, the nucleation process begins in the dead area.

## REFERENCES


1. Karelin F. N. *Obessolivanie vody obratnym osmosom* [Desalination of water by reverse osmosis. Moscow, Stroiizdat Publ., 1988. 208 p.].
2. Dytnerskii Iu. I. *Protsessy i apparaty khimicheskoi tekhnologii: Uchebnik dlia vuzov. Kniga 1* [Processes and apparatus of chemical engineering: Textbook for universities. Book 1. Moscow, Khimiia Publ., 1995. 400 p.].
3. Okazaki M., Kimura S. Scale formation on reverse osmosis membranes. *Journal of Chemical Engineering of Japan*, 1984, v. 17 (2), pp. 145–151.
4. Gilron J., Hasson D. Analysis of laminar flow precipitation fouling on reverse osmosis membranes, *Desalination*, 1986, v. 60, pp. 9–24.
5. Altena F. M., Belfort G., Otis T., Fiessinger F., Roveland T. M., Nicoletti T. Particle motion in a laminar slit flow: a fundamental fouling study. *Desalination*, 1980, v. 47, pp. 221–232.
6. Pervov A. Scale formation prognosis and cleaning procedure schedules in RO systems operation. *Desalination*, 1991, v. 83, pp. 77–118.
7. Salman M. A., Al-Nuwaibit G., Safar M., Al-Mesri A. Performance of physical treatment methods and different commercial antiscalants to control scaling deposition in desalination plant. *Desalination*, 2015, v. 369, pp. 18–25.
8. Jamaly S., Darwish N. N., Ahmed I., Hasan S. W. A short review on reverse osmosis pretreatment technologies // *Desalination*. 2014. v. 354. pp. 30–38.
9. Goh P. S., Lau W. J., Othman M. H. D., Ismail A. F. Membrane fouling in desalination and its mitigation strategies. *Desalination*, 2018, v. 425, pp. 130–155.
10. Jiang S., Li Y., Ladewig B. P. A review of reverse osmosis membrane fouling and control strategies. *Science of the Total Environment*, 2017, v. 595, pp. 567–583.
11. AL-Roomi Y. M., Hussain K. F. Potential kinetic model of scaling and scale inhibition mechanism // *Desalination*. 2016. v. 393. pp. 186–195.
12. Liu D., Dong W., Hiu F., Ledion J. Comparative performance of polyepoxysuccinic acid and polyaspartic acid on scaling inhibition by static and rapid controlled precipitation methods. *Desalination*, 2014, v. 304, pp. 1–10.
13. Shaussemier S. M. State of the art of natural inhibitors of calcium carbonate scaling. A review article. *Desalination*, 2015, v. 356, pp. 47–55.
14. Nir O. When does commercial software fail in predicting scaling tendency and what can we do better? The International Desalination Association World Congress. San Paulo, Brazil. 2017. REF: IDA 17 WC-58030_Nir.
15. Malki M. A novel calcium carbonate scaling model for maximum trecovery and inhibitor dosages in membrane systems. The International Desalination Association World Congress. San Paulo, Brazil. 2017. REF: IDA 17 WC-57993_Malki.
16. Li X., Hasson D., Shemer H. Flow conditions affecting the induction period of $CaSO_4$ scaling on RO membranes. *Desalination*, 2018, v. 431, pp. 119–125.
17. Pervov A. G. A simplified RO process design based on understanding of fouling mechanisms. *Desalination*, 1999, v. 126, pp. 227– 247.
18. Pervov A., Andrianov A., Danilycheva M. Preliminary evaluation of new green antiscalants for reverse osmosis water desalination. *Water Science and Technology: Water Supply*, 2017, v. 18 (1), pp. 167–174.
19. Pervov A., Andrianov A., Rudakova G., Popov K. A comparative study of some novel «green» and traditional antiscalants efficiency for the reverse osmotic Black Sea water desalination, *Desalination and Water Treatment*, 2017, v. 73, pp. 11–21.
20. Val C., Pervov A. G., Andrianov A. P., Golovesov V. A. [Investigation of antiscalant dosing influence on scaling process in reverse osmosis facilities and membrane surface adsorption]. *Vestnik MGSU*, 2019, v. 14 (6), pp. 722–733. (In Russian).
21. Kliachko V. A., Apel'tsin I. E. *Ochistka prirodnykh vod* [Natural water treatment. Moscow, Stroiizdat Publ., 1970. 580 p.].